

Article

# Dissecting $G_{q/11}$ -Mediated Plasma Membrane Translocation of Sphingosine Kinase-1

Kira Vanessa Blankenbach <sup>1,†</sup>, Ralf Frederik Claas <sup>1,†</sup>, Natalie Judith Aster <sup>1,†</sup>,  
Anna Katharina Spohner <sup>1</sup>, Sandra Trautmann <sup>2</sup>, Nerea Ferreirós <sup>2</sup> , Justin L. Black <sup>3</sup>,  
John J. G. Tesmer <sup>4</sup>, Stefan Offermanns <sup>5</sup>, Thomas Wieland <sup>6</sup>  and  
Dagmar Meyer zu Heringdorf <sup>1,\*</sup> 

<sup>1</sup> Institut für Allgemeine Pharmakologie und Toxikologie, Universitätsklinikum, Goethe-Universität, Theodor-Stern-Kai 7, 60590 Frankfurt am Main, Germany; kira.blankenbach@web.de (K.V.B.); frederik.claas@gmx.de (R.F.C.); s5599083@stud.uni-frankfurt.de (N.J.A.); spohner@em.uni-frankfurt.de (A.K.S.)

<sup>2</sup> Institut für Klinische Pharmakologie, Universitätsklinikum, Goethe-Universität, Theodor-Stern-Kai 7, 60590 Frankfurt am Main, Germany; trautmann@med.uni-frankfurt.de (S.T.); ferreirosbouzas@em.uni-frankfurt.de (N.F.)

<sup>3</sup> Department of Biochemistry and Biophysics, University of North Carolina, Chapel Hill, NC 27599, USA; justinblack8@gmail.com

<sup>4</sup> Departments of Biological Sciences and of Medicinal Chemistry and Molecular Pharmacology, Purdue University West Lafayette, West Lafayette, IN 47907-2054, USA; jtesmer@purdue.edu

<sup>5</sup> Abteilung für Pharmakologie, Max-Planck-Institut für Herz- und Lungenforschung, 61231 Bad Nauheim, Germany; offermanns.pharmacology@mpi-bn.mpg.de

<sup>6</sup> Experimentelle Pharmakologie Mannheim, European Center for Angioscience, Universität Heidelberg, 68167 Mannheim, Germany; thomas.wieland@medma.uni-heidelberg.de

\* Correspondence: heringdorf@med.uni-frankfurt.de; Tel.: +49-69-6301-3906

† These authors contributed equally to this work.

Received: 25 August 2020; Accepted: 27 September 2020; Published: 29 September 2020



**Abstract:** Diverse extracellular signals induce plasma membrane translocation of sphingosine kinase-1 (SphK1), thereby enabling inside-out signaling of sphingosine-1-phosphate. We have shown before that  $G_q$ -coupled receptors and constitutively active  $G_{\alpha_{q/11}}$  specifically induced a rapid and long-lasting SphK1 translocation, independently of canonical  $G_q$ /phospholipase C (PLC) signaling. Here, we further characterized  $G_{q/11}$  regulation of SphK1. SphK1 translocation by the  $M_3$  receptor in HEK-293 cells was delayed by expression of catalytically inactive G-protein-coupled receptor kinase-2, p63Rho guanine nucleotide exchange factor (p63RhoGEF), and catalytically inactive PLC $\beta_3$ , but accelerated by wild-type PLC $\beta_3$  and the PLC $\delta$  PH domain. Both wild-type SphK1 and catalytically inactive SphK1-G82D reduced  $M_3$  receptor-stimulated inositol phosphate production, suggesting competition at  $G_{\alpha_q}$ . Embryonic fibroblasts from  $G_{\alpha_{q/11}}$  double-deficient mice were used to show that amino acids W263 and T257 of  $G_{\alpha_q}$ , which interact directly with PLC $\beta_3$  and p63RhoGEF, were important for bradykinin  $B_2$  receptor-induced SphK1 translocation. Finally, an AIXXPL motif was identified in vertebrate SphK1 (positions 100–105 in human SphK1a), which resembles the  $G_{\alpha_q}$  binding motif, ALXXPI, in PLC $\beta$  and p63RhoGEF. After  $M_3$  receptor stimulation, SphK1-A100E-I101E and SphK1-P104A-L105A translocated in only 25% and 56% of cells, respectively, and translocation efficiency was significantly reduced. The data suggest that both the AIXXPL motif and currently unknown consequences of PLC $\beta$ /PLC $\delta$ (PH) expression are important for regulation of SphK1 by  $G_{q/11}$ .

**Keywords:** sphingosine kinase; sphingosine-1-phosphate; G-protein-coupled receptors;  $G_{\alpha_{q/11}}$

## 1. Introduction

Sphingosine-1-phosphate (S1P) is a multifunctional lipid mediator involved in organismal development and homeostasis of the immune, cardiovascular, nervous, and metabolic systems [1]. The metabolism of S1P is evolutionarily highly conserved, comprising sphingosine kinases (SphK), lipid phosphate phosphatases, S1P phosphatases, and S1P lyase [2]. In vertebrates, S1P activates five G-protein-coupled receptors (S1P-GPCRs), S1P<sub>1-5</sub> [3]. These receptors differentially couple to G<sub>i</sub>, G<sub>q/11</sub>, and G<sub>12/13</sub> proteins, and thereby regulate cell proliferation, survival, migration, adhesion, and Ca<sup>2+</sup>-dependent functions [1]. S1P-GPCRs are ubiquitously expressed and implicated for example in angiogenesis, maintenance of vascular tone and permeability, and immune cell trafficking. Accordingly, S1P-GPCRs play a role in autoimmunity, inflammation, fibrosis, and cancer [1]. Beyond these well-established effects of extracellular S1P, several roles and targets have been described for intracellular S1P. Examples include endocytic membrane trafficking [4,5], Ca<sup>2+</sup> mobilization, regulation of histone deacetylases, and mitochondrial respiration (reviewed in [6]). Of note, all of these studies show highly localized signaling by SphK, supporting the early conclusion that SphK localization is a key to function [7]. There are two SphK isoforms, which are derived from different genes and differ in tissue expression, structure, subcellular localization, regulation, and function. SphK2 has been observed in the cytosol, ER, mitochondria, and nucleus, whereas SphK1 is mainly found in the cytosol and may translocate to the plasma membrane upon stimulation [7–10]. Thus, SphK1 seems to be poised to generate S1P for cellular export, and thereby trigger S1P-GPCR cross-activation, which is known as inside-out signaling. A prominent example for inside-out signaling by S1P is observed in fibroblasts, in which SphK1 activation by platelet-derived growth factor (PDGF) leads to cross-activation of the S1P<sub>1</sub> receptor, which then mediates PDGF-induced cell migration [11]. Numerous other studies have shown the importance of the SphK/S1P axis for auto- and paracrine S1P signaling, and diverse transporters mediating S1P export have been identified (reviewed in [1,12]).

SphK1 is regulated transcriptionally, translationally, and post-translationally by many different pathways [8–10]. Acute activation of SphK1, with or without membrane translocation, can be induced by growth factors (for example PDGF, epidermal growth factor, nerve growth factor), cytokines (for example tumor necrosis factor- $\alpha$ , interleukin-1 $\beta$ , transforming growth factor- $\beta$ ), immunoglobulin receptors, or GPCRs (for review, see [8–10]). Several mechanisms have been described for plasma membrane translocation of SphK1. Phorbol-12-myristate-13-acetate (PMA)-induced translocation [13] involved phosphorylation of SphK1 at S225 by extracellular signal-regulated kinases (ERK)-1/2 [14]. In contrast, SphK1 translocation by oncogenic K-Ras was dependent on ERK but independent of S225 phosphorylation [15]. SphK1 translocation by both PMA and oncogenic Ras required calcium-and-integrin-binding-protein-1 (CIB1) [16]. Another pathway for acute activation and translocation of SphK1 is phosphatidic acid production [17]. Membrane binding of SphK1 has been attributed to a hydrophobic patch involving L194, F197, and L198 [4]. Furthermore, a highly positively charged site composed of K27, K29, and R186 was shown to form a single contiguous interface with the hydrophobic patch, mediating electrostatic interactions of SphK1 with membranes [18]. Finally, based on SphK1 crystal structures [19,20], Adams et al. have suggested that a dimeric quaternary structure may play a role in curvature-dependent targeting of SphK1 to the plasma membrane, and suggested how phosphorylation at S225 and protein binding to the C-terminus may potentially unmask membrane association determinants in SphK1 [21].

Our own studies have focused on regulation of SphK by GPCRs. Whereas overall SphK activity can be stimulated via G<sub>i</sub> as well as via G<sub>q</sub> pathways (reviewed in [22]), we have shown that specifically G<sub>q</sub>-coupled receptors induce a rapid and long-lasting translocation of SphK1 to the plasma membrane [23,24]. SphK1 translocation was further induced by overexpression of constitutively active G $\alpha_q$  and G $\alpha_{11}$ , but not G $\alpha_i$ , G $\alpha_{12}$ , or G $\alpha_{13}$  [23]. Importantly, G<sub>q</sub>-mediated SphK1 translocation was independent of phosphorylation at S225, because SphK1-S225A translocated after stimulation of the M<sub>3</sub> receptor in HEK-293 cells or the B<sub>2</sub> receptor in C2C12 myoblasts, similarly to the wild-type enzyme [23,25]. Classical G<sub>q/11</sub>/phospholipase C (PLC) signaling pathways were not involved in SphK1

targeting. Thus, neither cell-permeable diacylglycerol analogues or PMA, which induce activation of protein kinase C, nor thapsigargin or ionomycin, which induce increases in  $[Ca^{2+}]_i$ , were able to induce SphK1 translocation to the extent that it was induced by  $M_3$  receptor stimulation. Even a combined pretreatment with PMA plus ionomycin for about 8 min, which caused a minor SphK1 translocation by itself, did not prevent a subsequent marked SphK1 translocation stimulated by the  $M_3$  receptor. Furthermore, the involvement of  $Ca^{2+}$ /calmodulin, phospholipase D, tyrosine kinases, Rho kinase, and mitogen-activated protein kinase kinase was ruled out by specific inhibitors [23].

We, therefore, studied the regulation of SphK1 by  $G_{q/11}$  signaling pathways in more detail. We identified and characterized a motif conserved in vertebrate SphK1, with similarities to  $G_{\alpha_{q/11}}$  binding motifs in direct  $G_q$  effectors, which is required for  $G_q$ -mediated SphK1 translocation. We also showed that PLC $\beta$ , beyond its canonical downstream effectors, is important in inducing the most rapid membrane SphK1 translocation upon GPCR stimulation, and that this is mimicked by the pleckstrin homology (PH) domain of PLC $\delta_1$ .

## 2. Materials and Methods

### 2.1. Materials

Carbachol, bradykinin, and fatty-acid-free bovine serum albumin (BSA) were purchased from Sigma-Aldrich (Sigma-Aldrich Chemie GmbH, Taufkirchen, Germany). S1P was from Biomol GmbH (Hamburg, Germany). All other materials were from previously described sources [24,26].

### 2.2. Plasmids

The 3xHA-S1P $_1$  in pcDNA3.1 was obtained from the Missouri S&T cDNA Resource Center (Rolla, MO, USA).  $G_{\alpha_{q15}}$ -G66D was kindly provided by Dr. Evi Kostenis (University of Bonn, Bonn, Germany) [27]. The plasmid for expression of  $G_{\alpha_q}$ -YFP was a kind gift from Dr. Catherine Berlot (Weis Center for Research, Danville, PA, USA) [28]. Plasmids for expression of  $G_{\alpha_{i2}}$ ,  $G_{\alpha_q}$  wild-type,  $G_{\alpha_q}$ -Q209L-EE,  $G_{\alpha_q}$ -T257E,  $G_{\alpha_q}$ -Y261N,  $G_{\alpha_q}$ -W263D,  $G_{\alpha_q}$ -D321A,  $G_{\alpha_q}$ -Y356K,  $G_{\alpha_{15}}$ -Q212L-EE, G-protein-coupled-receptor-kinase-2 (GRK2)-K220R, and the bradykinin  $B_2$  receptor have been described previously [23,29–33].

Plasmids for expression of murine YFP-SphK1 (YFP-mSphK1), human GFP-SphK1 (GFP-hSphK1), human SphK1-G82D (hSphK1-G82D), and human mCherry-SphK1 (mCherry-hSphK1) have been described before [23,24]. Human SphK1-cerulean (hSphK1-cerulean) is a synthetic sequence with optimized codons (Mr. Gene, Regensburg, Germany) deduced from human SphK1 (GenBank accession number AF200328.1) and cerulean fluorescent protein (GenBank accession number ACO48272.1), which was cloned into the pcDNA3.1 vector using HindIII and XhoI. SphK1-F197A-L198Q-GFP and SphK1-L194Q-GFP were kindly provided by Dr. Pietro De Camilli (Yale University School of Medicine, New Haven, CT, USA) [4]. For experiments with the SphK1 mutants, mCherry-hSphK1-A100E-I101E and mCherry-hSphK1-P104A-L105A, these mutants and a second construct of mCherry-hSphK1 wild-type were designed according to the human SphK1 sequence described in GenBank accession number NM\_001142601.2. All three constructs were in pmCherry-C1 vector (Clontech/Takara Bio Europe, Saint-Germain-en-Laye, France) and obtained from Proteogenix (Schiltigheim, France). Full-length p63Rho guanine nucleotide exchange factor (p63RhoGEF) in pmCherry-C1 vector was a kind gift from Dr. Dorus Gadella (University of Amsterdam, Amsterdam, The Netherlands; Addgene plasmid #67896; <http://n2t.net/addgene:67896>; RRID:Addgene\_67896) [34]. PLC $\beta_3$  (GenBank accession number NM\_000932), C-terminally tagged with TurboGFP in pCMV6-AC-GFP vector, was obtained from OriGene Technologies (product #RG224268; Rockville, MD 20850, USA). PLC $\beta_3$ -H332A-GFP in pCMV6-AC-GFP vector was obtained from Proteogenix (Schiltigheim, France). PLC $\delta_1$ (PH)-CFP was a kind gift from Dr. Michael Schäfer (University of Leipzig, Leipzig, Germany) [35].

### 2.3. Cell Culture and Transfection

HEK-293 cells stably expressing the M<sub>3</sub> muscarinic acetylcholine receptor were cultured in Dulbecco's modified Eagle's medium (DMEM/F12) supplemented with 10% fetal calf serum, 100 U/mL penicillin G, and 0.1 mg/mL streptomycin as described [23]. Stock cultures of HEK-293 cells were grown in the presence of 0.5 mg/mL G418. Mouse embryonic fibroblasts (MEFs) from CIB1-deficient mice were made by J.L. Black in the laboratory of Dr. Leslie V. Parise (University of North Carolina at Chapel Hill, NC, USA) [36,37]. These MEFs, along with MEFs from G $\alpha_{q/11}$  double-deficient mice [38], were cultured in DMEM/F12 medium with 10% fetal calf serum, 100 U/mL penicillin G, and 0.1 mg/mL streptomycin. Transfection of HEK-293 cells was performed with Lipofectamine 2000 (Invitrogen GmbH, Karlsruhe, Germany), while MEFs were transfected with Turbofect (Fermentas, St. Leon-Rot, Germany) according to the manufacturer's instructions. For microscopy, the cells were seeded onto poly-L-lysine-coated 8-well slides ( $\mu$ -slide; ibidi GmbH, Martinsried, Germany). Before experiments, the cells were kept in serum-free medium overnight.

### 2.4. Measurement of SphK1 Translocation

SphK1 translocation was analyzed using fluorescently labelled SphK1 constructs and confocal laser scanning microscopy as described recently [24]. Cells grown on poly-L-lysine-treated 8-well slides ( $\mu$ -slide; ibidi GmbH, Martinsried, Germany) were incubated in Hank's balanced salt solution (HBSS) containing 118 mM NaCl, 5 mM KCl, 1 mM CaCl<sub>2</sub>, 1 mM MgCl<sub>2</sub>, 5 mM glucose, and 15 mM HEPES, pH 7.4. Fluorescence microscopy was performed with a Zeiss LSM510 Meta inverted confocal laser scanning microscope equipped with a Plan-Apochromat 63 $\times$ /1.4 oil immersion objective (Carl Zeiss MicroImaging GmbH, Göttingen, Germany). The following excitation (ex) laser lines and emission (em) filter sets were used: CFP and cerulean: ex 458 nm, em band-pass 465–510 nm; GFP: ex 488 nm, em long-pass 505 nm; GFP in combination with mCherry: ex 488 nm, em band-pass 505–530; YFP: ex 514, em band pass 525–600; mCherry: ex 561 nm, em band-pass 575–630 nm. Translocation half-times were determined by measuring the fluorescence intensity within defined cytosolic regions and fitting exponential functions to the translocation-induced decay in cytosolic fluorescence intensity. For estimation of translocation efficiency, the translocated fraction was calculated from these exponential curves as % decay in cytosolic fluorescence. While the average translocation half-time was ~5 s throughout all experiments, the translocated fraction values were comparatively variable between experiments because their calculation was influenced to a certain degree by cell shape changes. For quantification of SphK1 plasma membrane localization in cells co-transfected with G $\alpha_q$ -Q209L-EE (Figure 6G,H), we measured the fluorescence profiles of individual cells using the ZEN software (Carl Zeiss MicroImaging GmbH, Göttingen, Germany), and calculated the ratios of plasma membrane and cytosolic fluorescence intensities.

### 2.5. Inositol Phosphate Production

Inositol phosphate production was measured as described recently [24]. Briefly, HEK-293 cells labelled with 1  $\mu$ Ci/mL myo-2-[<sup>3</sup>H]-inositol (23.75 Ci/mmol; Perkin Elmer Life and Analytical Sciences, Rodgau-Jügesheim, Germany) were stimulated with 100  $\mu$ M carbachol in HBSS containing LiCl for 20 min at 37 °C. The reaction was stopped by addition of 2 mL ice-cold methanol. The cells were scraped from the dishes, 1 mL H<sub>2</sub>O and 2 mL chloroform were added, and the aqueous phase was transferred to Poly-Prep AG 1-X8 columns (Bio-Rad, Hercules, CA, USA). After washing with H<sub>2</sub>O and 50 mM ammonium formate, inositol phosphates were eluted with 5 mL of 1 M ammonium formate and 0.1 M formic acid. The radioactivity was measured by liquid scintillation counting.

### 2.6. Western Blotting

Cells grown to near confluence on 6 cm-dishes were lysed, the proteins were separated by SDS gel electrophoresis and blotted onto polyvinylidene difluoride membranes. The SphK1 antibody,

directed against the C-terminus of human SphK1, was a kind gift from Drs. Andrea Huwiler (University of Bern, Bern, Switzerland) and Josef Pfeilschifter (Goethe-University Frankfurt, Frankfurt, Germany) [39]. Anti-mCherry antibody (ab125096) was from Abcam (Cambridge, UK). Anti- $\beta$ -actin (A5441) was from Sigma-Aldrich Chemie GmbH (Taufkirchen, Germany), HRP-conjugated secondary antibodies were from GE Healthcare (Freiburg, Germany), and the enhanced chemiluminescence system was from Millipore Corporation (Billerica, MA, USA).

### 2.7. High-Performance Liquid Chromatography Tandem Mass Spectrometry

S1P (d18:1) concentrations were determined by high-performance liquid chromatography tandem mass spectrometry as described recently [24].

### 2.8. Data Analysis and Presentation

Fluorescence images were edited with the ZEN software (Carl Zeiss MicroImaging GmbH, Göttingen, Germany). Statistical tests, curve fitting, and calculations of translocation half-times were done with Prism-5 (GraphPad Software, San Diego, California, USA). Averaged data are expressed as means  $\pm$  SD or means  $\pm$  SEM from the indicated number ( $n$ ) of cells, samples, or experiments, respectively.

## 3. Results and Discussion

Similar to our previous publications [23,25], we observed a rapid and long-lasting translocation of both murine and human SphK1 to the plasma membrane upon stimulation of the  $M_3$  muscarinic acetylcholine receptor in HEK-293 cells (Figures 1, 2, 5, and 6). To confirm the involvement of  $G_{\alpha_{q/11}}$  in this system, we analyzed the influence of a catalytically inactive mutant of GRK2, GRK2-K220R. GRK2-K220R is unable to phosphorylate G protein-coupled receptors but directly binds  $G_{\alpha_{q/11}}$  and  $G\beta\gamma$ , and acts as a  $G_{\alpha_{q/11}}/G\beta\gamma$  scavenger [29] (see also [40]). When co-expressed with YFP-mSphK1, GRK2-K220R strongly delayed, reduced, and in several cells even fully prevented translocation of the enzyme by the  $M_3$  receptor (Figure 1A–C). Together with our previous observation that constitutively active  $G_{\alpha_q}$  induced SphK1 translocation, this result indicated that  $M_3$  receptor-induced translocation was mediated by  $G_{\alpha_q}$ .

Another binding partner and direct effector of  $G_{\alpha_{q/11}}$  is p63RhoGEF [41,42]. It is known that p63RhoGEF activates RhoA but also competes with PLC $\beta$  for activated  $G_{\alpha_{q/11}}$ , and vice versa [41]. Therefore, we tested the influence of p63RhoGEF on SphK1 translocation. As shown in Figure 1D–F, overexpressed mCherry-p63RhoGEF strongly delayed and reduced  $M_3$  receptor-induced translocation of GFP-hSphK1. This result indicated that SphK1 is not activated by p63RhoGEF downstream signaling and matches our previous observation that a Rho kinase inhibitor did not prevent  $G_{q/11}$ -mediated SphK1 translocation [23]. The data obtained with GRK2-K220R and p63RhoGEF can be explained by competition of the different  $G_{\alpha_{q/11}}$  effectors for binding at the active  $G_{\alpha_q}$  or  $G_{\alpha_{11}}$  subunit. Thus, the data suggest two possibilities: (1) that SphK1 is activated downstream of PLC $\beta$ , and (2) that SphK1 directly interacts with and is translocated by active  $G_{\alpha_{q/11}}$ . To analyze these possibilities further, we next tested the influence of PLC $\beta$  on SphK1 translocation.

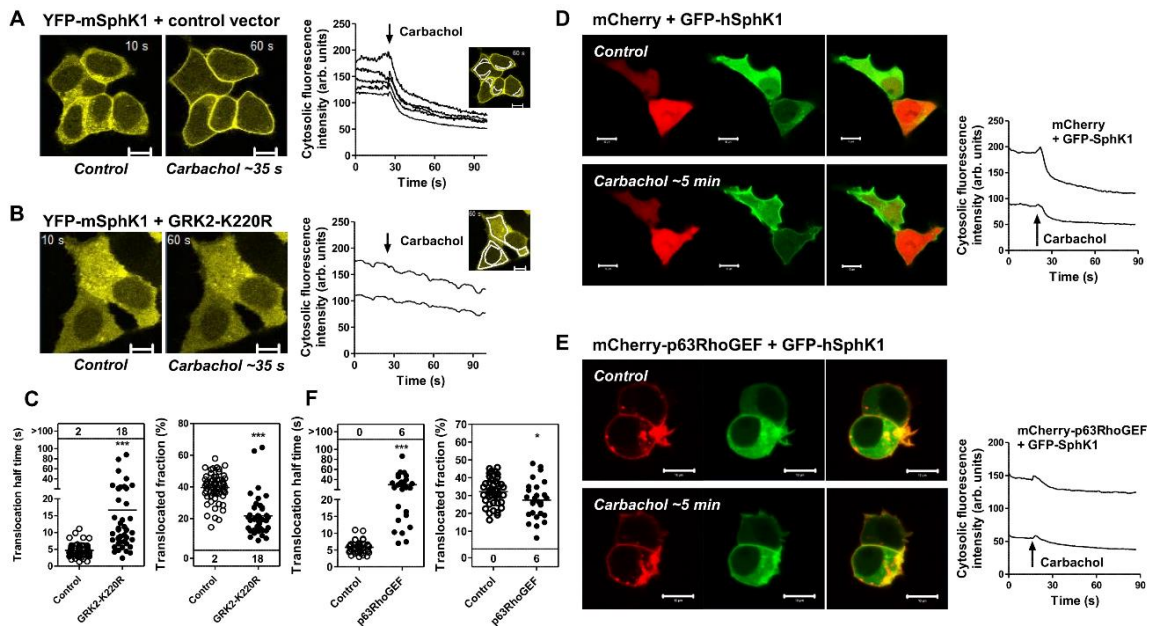


**Figure 1.** Influence of catalytically inactive GRK2 and p63RhoGEF on  $M_3$  receptor-induced SphK1 translocation. HEK-293 cells stably expressing the  $M_3$  muscarinic acetylcholine receptor were transfected as indicated and translocation of SphK1 was monitored by live cell imaging with a confocal laser scanning microscope. (A–C) Cells were transfected with YFP-mSphK1 and either catalytically inactive GRK2 (GRK2-K220R) or control vector. Time series were acquired with  $\sim 3$  images/s and  $100 \mu\text{M}$  carbachol was added after  $\sim 25$  s. Images were taken from representative time series at 10 and 60 s, thus showing localization of YFP-mSphK1 before and  $\sim 35$  s after stimulation with carbachol, respectively. The line graphs show the corresponding time courses of cytosolic fluorescence intensity, measured in the indicated cytosolic regions. (C) The SphK1 translocation half-times were measured by fitting exponential curves to the translocation-induced decay in cytosolic fluorescence intensity. Each dot represents a single cell. Translocation half-times  $>100$  depict the number of cells which did not respond. Note: \*\*\*  $p < 0.0001$  in  $t$ -tests with Welch's correction for unequal variances. (D–F) Cells were transfected with GFP-hSphK1 (green) and either mCherry or mCherry-p63RhoGEF (red). Representative images were taken at high spatial resolution immediately before and after the acquisition of time series, during which only GFP fluorescence was monitored with 1 image/s. The line graphs showing time courses of cytosolic fluorescence intensity correspond to the cells shown in the images. Carbachol was added at the indicated time points. (F) SphK1 translocation half-time was measured as described in (C). Note: \*  $p < 0.05$ , \*\*\*  $p < 0.0001$  in  $t$ -tests with Welch's correction for unequal variances. Micrometer bars,  $10 \mu\text{m}$ .

As shown in Figure 2A–D, overexpression of catalytically inactive PLC $\beta_3$ -H332A-GFP caused a significant delay in  $M_3$  receptor-induced translocation of mCherry-hSphK1. In contrast, wild-type PLC $\beta_3$ -GFP slightly but significantly accelerated translocation of mCherry-hSphK1. While the inhibitory effect of PLC $\beta_3$ -H332A could be caused both by competition at  $G\alpha_q$  and by its activity as a GTPase-activating protein (GAP), the acceleration by wild-type PLC $\beta_3$  shows that its GAP activity was surmounted by its stimulatory effect. Interestingly, acceleration of  $M_3$  receptor-induced SphK1 translocation was also observed upon expression of the PH domain of PLC $\delta_1$ , which serves as a sensor for phosphatidylinositol-4,5-bisphosphate (PI(4,5)P $_2$ ) [43]. As described [35,43], PLC $\delta_1$ (PH)-CFP was localized at the plasma membrane in unstimulated cells and rapidly translocated to the cytosol after stimulation of the  $M_3$  receptor (Figure 2E). The velocity of PLC $\delta_1$ (PH)-CFP translocation was not altered by co-expression of YFP-mSphK1; however, translocation of YFP-mSphK1 was significantly accelerated by co-expression of PLC $\delta_1$ (PH)-CFP (Figure 2F). Since the PH domain of PLC $\delta_1$  does not induce DAG and IP $_3$  production, its effect on SphK1 is rather due to PI(4,5)P $_2$  binding or other cellular effects, for example competition with other PI(4,5)P $_2$  binding proteins. In fact, PLC $\delta_1$ (PH) has been

shown to reduce the amount of phosphatidylinositol-4-phosphate-5-kinase (PIP5K) at the plasma membrane, and thereby the cellular level of PI(4,5)P<sub>2</sub> [44]. According to this report, expression of PLCδ<sub>1</sub>(PH) will rather decrease than increase PLCβ catalytic activity, but nevertheless accelerated SphK1 translocation. Importantly, RhoA, the downstream effector of p63RhoGEF, activates type I PIP5K [45]. Thus, it is possible that (over)expression of PLCβ<sub>3</sub> or PLCδ<sub>1</sub>(PH) accelerated SphK1 translocation while p63RhoGEF delayed SphK1 translocation by decreasing and enhancing PI(4,5)P<sub>2</sub> levels, respectively. However, other tools manipulating PI(4,5)P<sub>2</sub> levels such as the multiple pathway inhibitor genistein [46] did not alter SphK1 translocation velocity in our cells ([23] and data not shown). Consequently, the mechanisms by which (over)expression of PLCβ<sub>3</sub> and PLCδ<sub>1</sub>(PH) accelerate SphK1 translocation remain unclear.

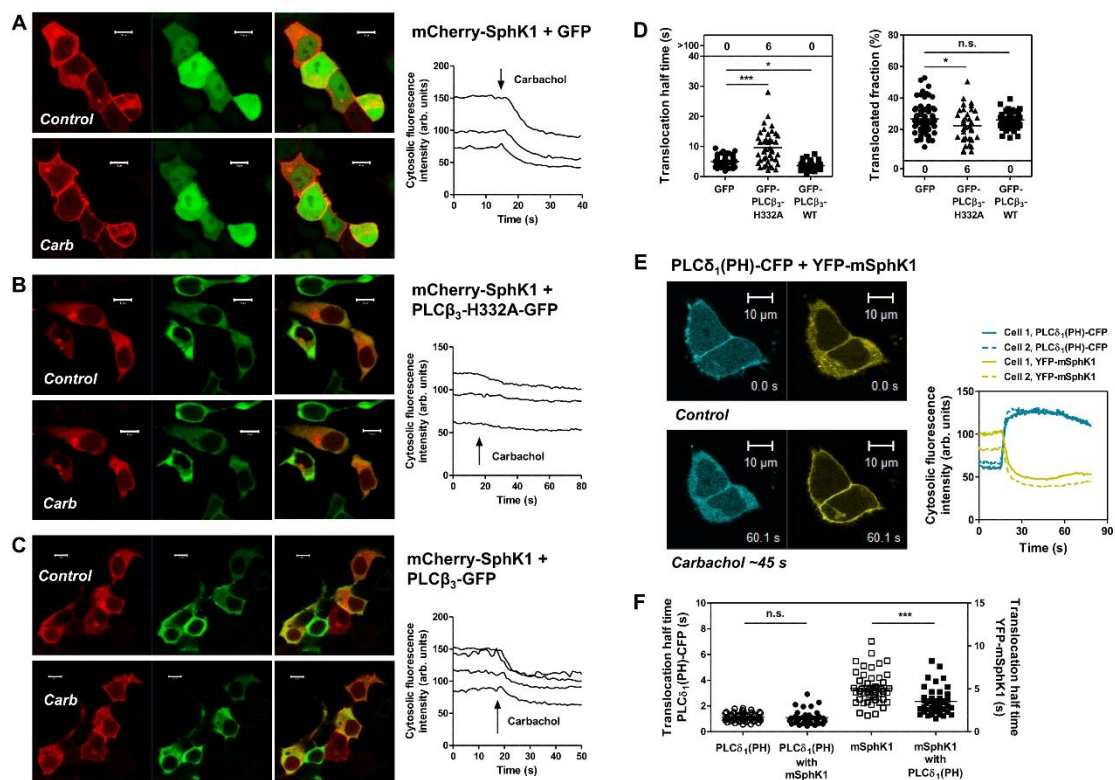


**Figure 2.** Influence of PLCβ<sub>3</sub> and PLCδ(PH) on M<sub>3</sub> receptor-induced SphK1 translocation. HEK-293 cells stably expressing the M<sub>3</sub> receptor were transfected as indicated. (A–D) Cells were transfected with mCherry-hSphK1 (red) and GFP (A), catalytically inactive PLCβ<sub>3</sub> (PLCβ<sub>3</sub>-H332A-GFP) (B) or PLCβ<sub>3</sub> wild-type (PLCβ<sub>3</sub>-WT) (C). Representative images were taken at high spatial resolution immediately before and after the acquisition of time series during which only mCherry fluorescence was monitored at 1 image/s. The line graphs showing time courses of cytosolic fluorescence intensity correspond to the cells shown in the images. Carbachol was added at the indicated time points. (D) SphK1 translocation half-times were measured by fitting exponential curves to the decay in cytosolic fluorescence. The translocated fraction represents the decay in cytosolic fluorescence intensity in % of initial fluorescence. Each dot represents a single cell. Translocation half-times >100 depict the number of cells which did not respond. Note: n.s., not significant; \*  $p < 0.05$ , \*\*\*  $p < 0.0001$  in  $t$ -tests with Welch’s correction for unequal variances. (E,F) Cells were transfected with PLCδ(PH)-CFP (cyan), YFP-mSphK1 (yellow), or both. Carbachol-induced translocation of the two proteins was studied in time series with ~3–4 images/s. (E) Images were taken from a representative time series with double-transfected cells before and ~45 s after addition of carbachol. The line graph shows the time course of cytosolic fluorescence intensity for both CFP and YFP. (F) Translocation half-times for PLCδ(PH)-CFP and YFP-mSphK1, both alone and in combination. Note: n.s., not significant; \*\*\*  $p < 0.0001$  in  $t$ -tests with Welch’s correction for unequal variances. Micrometer bars, 10 μm.

Interestingly, not all members of the  $G\alpha_q$  subfamily ( $G\alpha_q$ ,  $G\alpha_{11}$ ,  $G\alpha_{14}$ , and  $G\alpha_{15/16}$ , with  $G\alpha_{15}$  being the murine homologue of human  $G\alpha_{16}$ ) interact with the established targets in the same manner. For example,  $G\alpha_{15/16}$  does not bind to GRK2, and binds to but does not activate p63RhoGEF (reviewed in [40]). With the aim of possibly separating PLC $\beta$  activation and SphK1 translocation, we expressed constitutively active  $G\alpha_{15}$ -Q212L-EE and studied its influence on SphK1 localization. As shown in Figure 3A, mCherry-SphK1 was strongly localized at the plasma membrane in  $G\alpha_{15}$ -Q212L-EE-transfected cells. Thus, PLC $\beta$  activation and SphK1 translocation could not be separately targeted by using  $G\alpha_{15/16}$ .

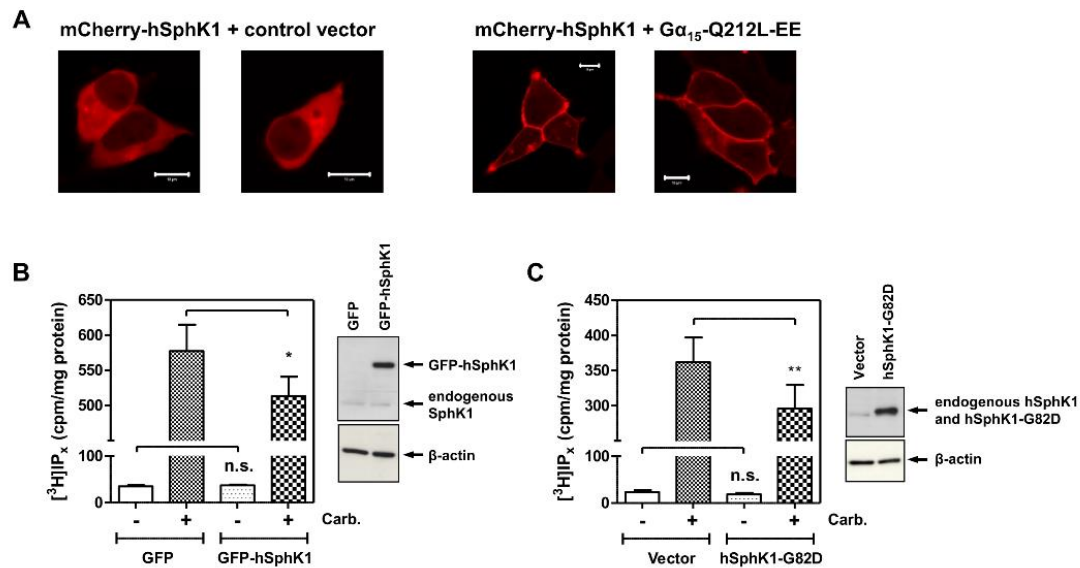


**Figure 3.** (A) SphK1 translocation by constitutively active  $G\alpha_{15}$ . HEK-293 cells stably expressing the  $M_3$  receptor were transfected with mCherry-hSphK1 and either control vector or  $G\alpha_{15}$ -Q212L-EE. Shown are two representative images each. Bars, 10  $\mu$ m. (B,C) Influence of SphK1 overexpression on  $M_3$  receptor-induced inositol phosphate production. HEK-293 cells were transfected with GFP or GFP-hSphK1 (B), or with the pcDNA3.1 vector or hSphK1-G82D (C). The formation of [ $^3$ H]inositol phosphates ([ $^3$ H]IP<sub>x</sub>) was measured in [ $^3$ H]inositol-labelled cells stimulated with 100  $\mu$ M carbachol (Carb.) for 20 min in the presence of LiCl. The expression of GFP-hSphK1 and hSphK1-G82D was confirmed with an anti-SphK1 antibody. The data are means  $\pm$  SEM from  $n = 9$  (B) or  $n = 8$  (C) independent experiments, each performed in triplicate. Note: n.s., not significant; \*  $p < 0.05$ , \*\*  $p = 0.01$  in paired  $t$ -test.

To further analyze the mutual interactions of SphK1 and PLC $\beta$ , we next studied the influence of overexpressed SphK1 on  $M_3$  receptor-induced accumulation of [ $^3$ H]inositol phosphates in [ $^3$ H]inositol-labelled cells. As shown in Figure 3B, GFP-SphK1 had no influence on basal inositol phosphate production, but significantly reduced  $M_3$  receptor-stimulated inositol phosphate production. Moreover, SphK1-G82D, which is a catalytically inactive mutant [47], had the same effect (Figure 3C), indicating that it was due to protein–protein interactions and independent of S1P signaling. This result indeed suggests that SphK1 competed with PLC $\beta$  for  $G\alpha_{q/11}$  in the context of a living cell, although it remains possible that SphK1 binds to PLC $\beta$ , thereby reducing its activity.

Next, we used embryonic fibroblasts from mice deficient in both  $G\alpha_q$  and the related  $G\alpha_{11}$  [38] to study structural requirements of  $G\alpha_{q/11}$  for inducing SphK1 translocation. In  $G\alpha_{q/11}$  double-deficient MEFs, both hSphK1-cerulean and YFP-mSphK1 were localized in the cytosol, and their localization did not change upon stimulation of the  $B_2$  bradykinin receptor unless  $G\alpha_q$ -YFP or  $G\alpha_q$  wild-type were co-transfected (Figure 4). Of note, in cells expressing  $G\alpha_q$  wild-type or  $G\alpha_q$ -YFP, SphK1 was localized to a small part at the plasma membrane, even under control conditions (Figure 4B,E). This was not the case in cells lacking both  $G\alpha_q$  and  $G\alpha_{11}$  (Figure 4A,D). Using these cells, we confirmed

that stimulation of the  $G_i$ -coupled  $S1P_1$  receptor did not induce SphK1 translocation, even when  $S1P_1$ , GFP-hSphK1, and  $G\alpha_{i2}$  were co-transfected (Figure 4C). However, expression of the chimeric G-protein,  $G\alpha_{q15}$ -G66D, which links  $G_i$ -coupled receptors to  $G_q$  signaling pathways [27], enabled  $S1P_1$  to induce SphK1 translocation (Figure 4C). In cells co-expressing the  $B_2$  receptor, YFP-mSphK1, and  $G\alpha_q$  wild-type, 10  $\mu$ M bradykinin induced translocation of SphK1 with an average half-time of  $5.8 \pm 0.6$  s (mean  $\pm$  SEM,  $n = 31$  cells; Figure 4E,G). Several  $G\alpha_q$  mutants were able to fully restore  $B_2$  receptor-induced SphK1 translocation in  $G\alpha_{q11}$  double-deficient MEFs, with translocation half-times that did not significantly differ from that of  $G\alpha_q$  wild-type. These were  $G\alpha_q$ -Y261N ( $t_{1/2} = 7.9 \pm 1.4$  s,  $n = 17$ ),  $G\alpha_q$ -D321A ( $t_{1/2} = 4.1 \pm 0.5$  s,  $n = 14$ ), and  $G\alpha_q$ -Y356K ( $t_{1/2} = 4.5 \pm 0.5$  s,  $n = 17$ ) (all means  $\pm$  SEM; Figure 4G). In cells expressing  $G\alpha_q$ -W263D,  $B_2$  receptor-stimulated SphK1 translocation was significantly delayed, with a half-time of  $10.8 \pm 1.1$  s (mean  $\pm$  SEM,  $n = 18$  cells; Figure 4G). Importantly, SphK1 translocation was very slow in cells expressing  $G\alpha_q$ -T257E and typically visible only after 2–3 min, for which reason the average translocation half-time was not determined (Figure 4F). Taken together, the amino acids T257 and W263 of  $G\alpha_q$  are important for targeting of SphK1. Interestingly,  $G\alpha_q$ -T257,  $G\alpha_q$ -Y261, and  $G\alpha_q$ -W263 are implicated in  $G\alpha_q$ /GRK2 interaction, as mutation of these residues abolished  $G\alpha_q$  binding to GRK2 [31,48]. Furthermore, PLC $\beta$  activation was completely inhibited by mutation of  $G\alpha_q$ -R256/T257 to alanines [49]. Finally, mutants  $G\alpha_q$ -Y261N and  $G\alpha_q$ -W263D had reduced binding to p63RhoGEF, while  $G\alpha_q$ -T257E neither bound nor activated p63RhoGEF [33]. Thus, amino acid T257 of  $G\alpha_q$  plays a major role in binding or activation of PLC $\beta$ , p63RhoGEF, and GRK2, and likewise is important for SphK1 translocation. This result is in agreement with both hypotheses: (1) that SphK1 is activated downstream of PLC $\beta$ , and (2) that SphK1 competes with PLC $\beta$ , p63RhoGEF, and GRK2 for the same  $G\alpha_q$  binding site.

Next, we wondered which structural elements in SphK1 were required for  $G\alpha_q$ -mediated translocation of the enzyme. As described above, SphK1 membrane translocation by PMA and oncogenic Ras involved CIB1, which binds to the calmodulin binding site of SphK1 [16,50]. Amino acids L194, F197, and L198 of hSphK1 were important for CIB1 binding, and the double mutant hSphK1-F197A-L198Q had reduced CIB1 binding and did not translocate to the plasma membrane in response to PMA, while its catalytic activity remained nearly intact [16,50]. Another study localized L194, F197, and L198 within a hydrophobic patch on the surface of SphK1 and demonstrated that hSphK1-L194Q and hSphK1-F197A-L198Q did not bind to acidic liposomes *in vitro* and were not recruited to tubular membrane invaginations induced by cholesterol extraction in living cells [4]. Hence, this hydrophobic patch is regarded as essential for curvature-sensitive membrane binding of SphK1 [9,21]. We show here that the two hSphK1 mutants, hSphK1-L194Q-GFP and hSphK1-F197A-L198Q-GFP, did not visibly translocate to the plasma membrane in response to  $M_3$  receptor activation in HEK-293 cells (Figure 5A–C). Interestingly, while usually there were only low levels of wild-type SphK1 in the nuclei of transfected HEK-293 cells, there was significant fluorescence in the nuclei of cells transfected with hSphK1-L194Q-GFP (Figure 5B). Furthermore, the mutant, hSphK1-F197A-L198Q-GFP, was strongly localized to the nuclei, with some cells expressing even more fluorescence in the nucleus than in the cytoplasm (Figure 5C). This observation suggests that mutations in this region might possibly disrupt a nuclear export sequence, although the two known nuclear export sequences in hSphK1 comprise amino acids 147–155 and 161–169 [51]. Because of the mentioned involvement of hSphK1-L194, -F197, and -L198 in CIB1 binding [16], we furthermore studied  $G_{q11}$ -dependent SphK1 translocation in CIB1-deficient MEFs. As shown in Figure 5D, the  $B_2$  receptor was clearly able to induce GFP-hSphK1 translocation in cells lacking CIB1. In addition, the translocation half-time was not altered (data not shown). Taken together, we demonstrate that this region comprising L194, F197, and L198 in hSphK1 is important for  $G_{q11}$ -dependent SphK1 translocation, very likely because this hydrophobic patch is required for membrane binding. CIB1, however, does not play a role in  $G_q$ -mediated SphK1 translocation.

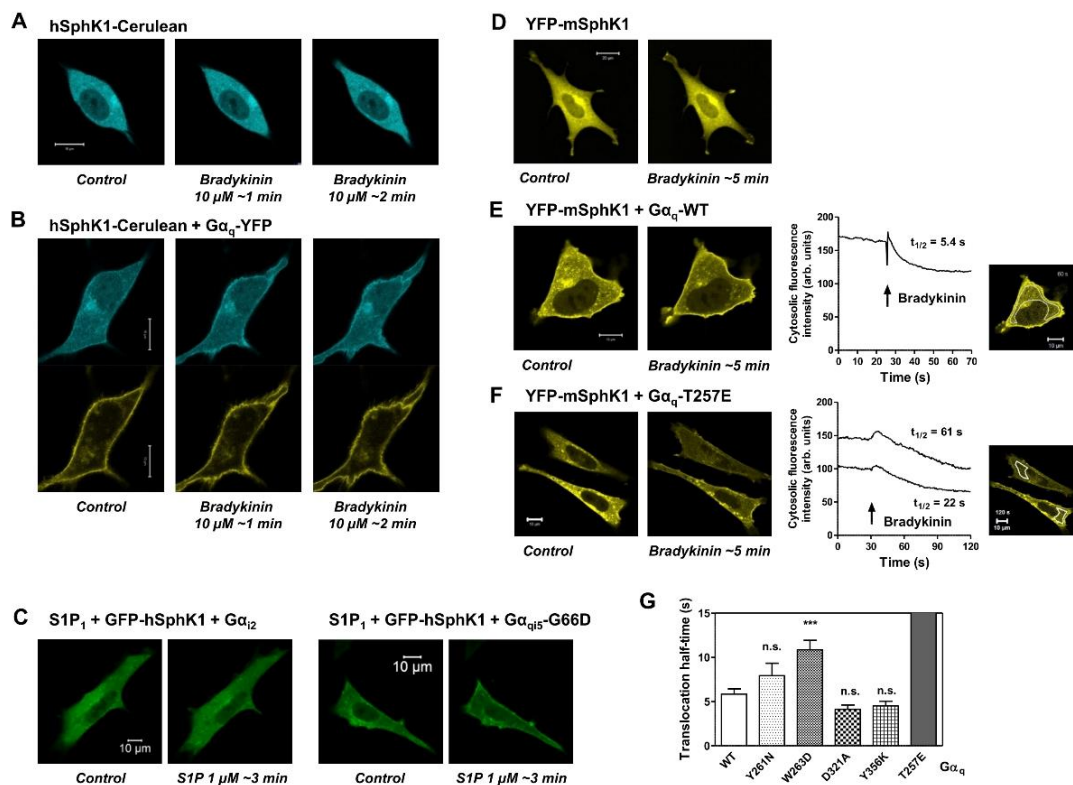


**Figure 4.** Identification of G $\alpha_q$  residues required for G $_{q/11}$ -mediated SphK1 translocation. (A–G) SphK1 translocation was analyzed in G $\alpha_{q/11}$ -double-deficient MEFs. (A,B) The cells were co-transfected with the bradykinin B<sub>2</sub> receptor and hSphK1-cerulean without (A) and with (B) G $\alpha_q$ -YFP. Images were taken before and after addition of 10  $\mu$ M bradykinin as indicated. (C) The cells were co-transfected with the S1P<sub>1</sub> receptor, GFP-hSphK1, and either G $\alpha_{i2}$  or G $\alpha_{q15}$ -G66D as indicated. Images were taken before and ~3 min after addition of 1  $\mu$ M S1P. (D–G) The cells were co-transfected with the B<sub>2</sub> receptor, YFP-mSphK1, and G $\alpha_q$  wild-type (G $\alpha_q$ -WT) or various G $\alpha_q$  mutants as indicated. Images were taken at a high resolution before and ~5 min after addition of 10  $\mu$ M bradykinin. The time course of SphK1 translocation was measured by taking series of images at lower spatial resolution at ~1 image/400 ms. Cytosolic fluorescence intensity was measured in selected regions as indicated in the inserts in (E,F), and translocation half-times were calculated by fitting exponential curves to the decay in the cytosolic fluorescence intensity. (G) Translocation half-times obtained with the various G $\alpha_q$  mutants. Data are means  $\pm$  SEM;  $n = 31$  (G $\alpha_q$ -WT);  $n = 14$ –18 (G $\alpha_q$  mutants). Note: n.s., not significant; \*\*\*  $p < 0.0001$  in one-way ANOVA followed by Bonferroni’s post-test. The micrometer bars represent 10  $\mu$ m.

PLC $\beta$  and p63RhoGEF bind to the effector binding site of G $\alpha_q$  primarily via their conserved ALXXPI motifs (X represents any amino acid) [40]. Although both enzymes have additional domains that contribute to the interaction with active G $\alpha_q$ , mutation of the conserved leucine in this motif (L859 in human PLC $\beta_3$ , L475 in human p63RhoGEF) is sufficient to eliminate G $\alpha_q$  binding [40]. Similarly, although GRK2 lacks the ALXXPI motif, it contains a structurally equivalent leucine (L118) that is essential for G $\alpha_q$  binding [40]. Interestingly, there is a similar motif, AIXXPL, in vertebrate SphK1, with isoleucine instead of leucine in position 2 and leucine instead of isoleucine in position 6 of this motif (Figure 6A). Comparison of different SphK1 homologues shows the conservation of this motif among vertebrates, with small variations concerning the leucine/isoleucine substitutions, such as ALXXPL in *Gallus gallus* and AIXXPI in *Xenopus laevis* (Figure 6A). We did not find such a motif in non-vertebrate SphK, such as *Drosophila melanogaster* or *Caenorhabditis elegans* SphK, in agreement with the current view that S1P-GPCRs, which are ultimately targeted by SphK1 plasma membrane translocation, have evolved with the vertebrates (see [1]). To study the functional importance of the AIXXPL motif, we generated the mutants hSphK1-A100E-I101E and

hSphK1-P104A-L105A as fusion proteins with *N*-terminal mCherry. When expressed in HEK-293 cells, both mCherry-hSphK1-A100E-I101E and mCherry-hSphK1-P104A-L105A were detected by an anti-mCherry antibody and by an antibody directed against the C-terminus of human SphK1, and had the same molecular weight as mCherry-hSphK1 wild-type (Figure 6B). The double bands seen in Figure 6 were also seen with mCherry alone, and thus caused by the fluorescent tag (Figure 6B). Furthermore, expression of all the SphK1 mutants elevated intracellular S1P concentrations, as measured by high-performance liquid chromatography tandem mass spectrometry. In cells transfected with mCherry, the concentration of S1P was  $1050 \pm 150$  pg/mg protein ( $n = 8$ ), while expression of mCherry-hSphK1 wild-type increased S1P to  $1500 \pm 200$  pg/mg protein ( $n = 6$ ;  $p < 0.001$ ). Cells expressing mCherry-hSphK1-A100E-I101E had S1P concentrations of  $1300 \pm 160$  pg/mg protein ( $n = 9$ ;  $p < 0.05$ ), and cells expressing mCherry-hSphK1-P104A-L105A had  $1500 \pm 190$  pg/mg protein ( $n = 9$ ;  $p < 0.001$ ) (all values represent means  $\pm$  SD, with significance tested in one-way ANOVA). These results indicated that all of the mutants were catalytically active.

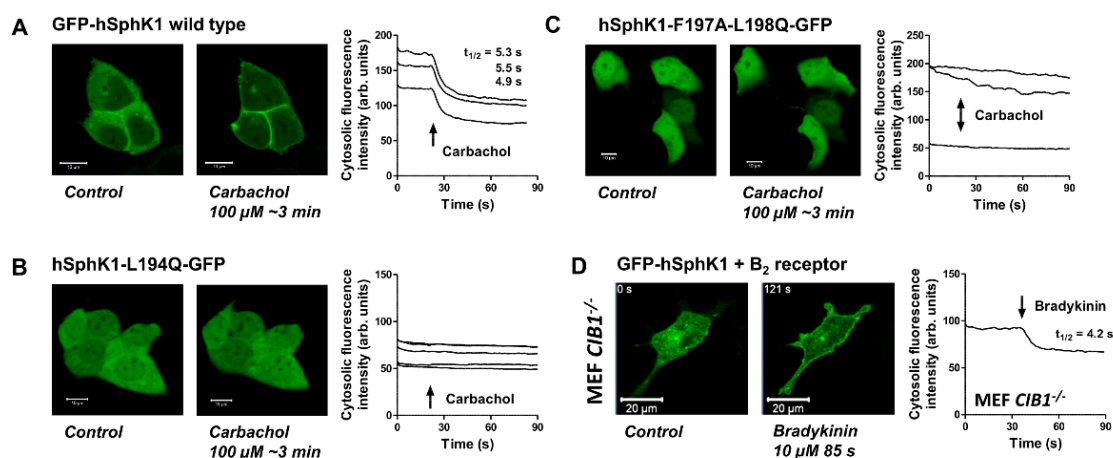


**Figure 5.** Role of the hydrophobic patch in SphK1 for  $G_{q/11}$ -mediated SphK1 translocation. (A–C) HEK-293 cells stably expressing the  $M_3$  receptor were transfected with GFP-hSphK1, hSphK1-L194Q-GFP, or hSphK1-F197A-L198Q-GFP. Translocation of SphK1 mutants was studied upon stimulation of the cells with  $100 \mu\text{M}$  carbachol. Shown are images before and after stimulation, and time courses of cytosolic fluorescence from representative experiments. In (C), the cytosolic fluorescence of the cell in the upper left could not be evaluated because of the strong change in cell shape. The micrometer bars represent  $10 \mu\text{m}$ . (D) Role of CIB1 for  $G_q$ -mediated SphK1 translocation. MEFs from CIB1-deficient mice were transfected with GFP-hSphK1 and the  $B_2$  receptor. Shown are images and time courses of cytosolic fluorescence from a representative time series during which  $10 \mu\text{M}$  bradykinin was added after 35 s. The two images, thus, show localization of GFP-hSphK1 before and 85 s after addition of bradykinin. Micrometer bars,  $20 \mu\text{m}$ .

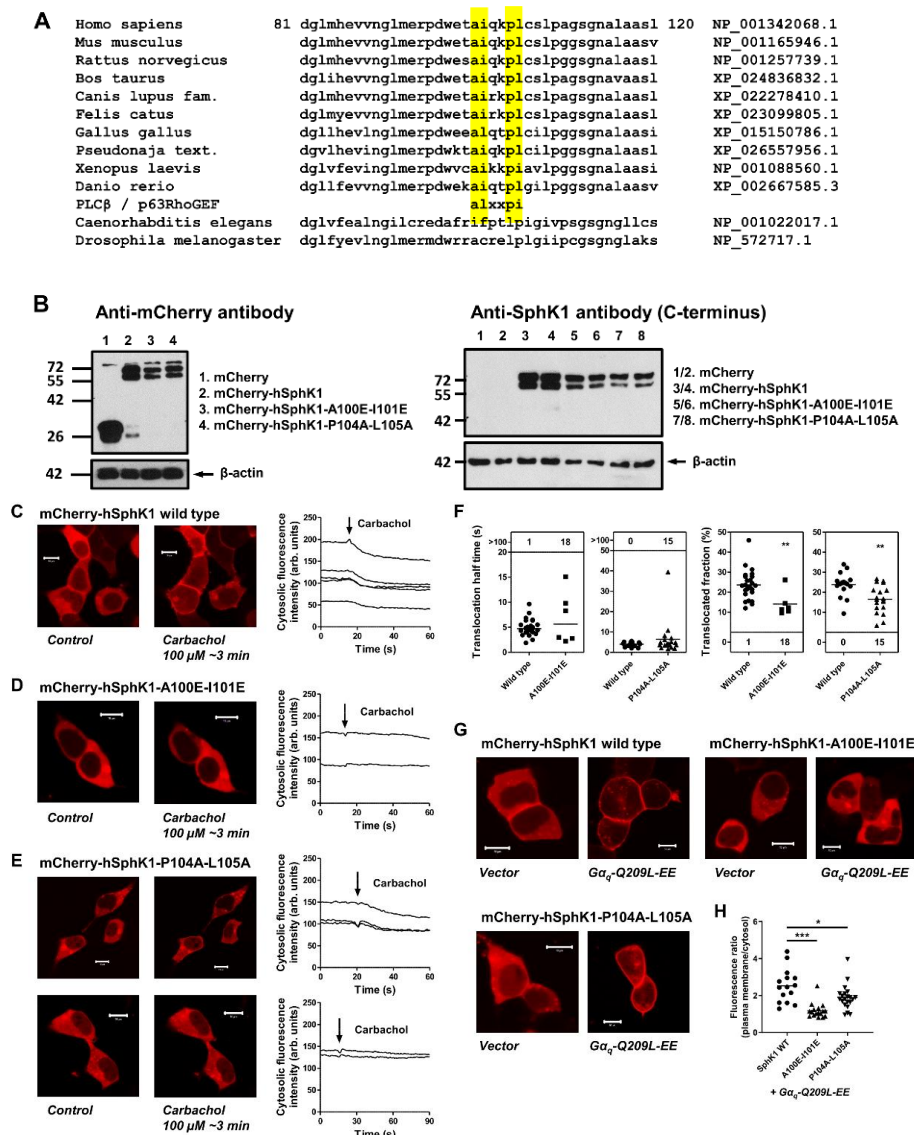


**Figure 6.** Identification of structural elements in SphK1 required for G<sub>q/11</sub>-mediated translocation. (A) Sequence alignment of diverse SphK1 homologues between amino acids 81–120 of human SphK1. (B) Western blot analysis of mCherry-hSphK1-A100E-I101E and mCherry-hSphK1-P104A-L105A expressed in HEK-293 cells. (C–E) Analysis of localization and translocation of mCherry-hSphK1-A100E-I101E and mCherry-hSphK1-P104A-L105A in HEK-293 cells stably expressing the M<sub>3</sub> receptor. The cells were stimulated with 100 μM carbachol as indicated. Shown are images before and after stimulation, and time courses of cytosolic fluorescence from representative experiments. Since translocation of mCherry-hSphK1-P104A-L105A was variable, two examples are shown here for this mutant. (F) Summary of translocation half-times and translocated fractions from (C–E). Each dot represents a single cell. Translocation half-times >100 depict the number of cells which did not respond. Note: \*\* *p* < 0.01 in unpaired *t*-test. (G,H) Influence of constitutively active Gα<sub>q</sub> on subcellular localization of hSphK1 mutants. HEK-293 cells were transfected with mCherry-hSphK1 wild-type, mCherry-hSphK1-A100E-I101E, or mCherry-hSphK1-P104A-L105A, plus either control vector or Gα<sub>q</sub>-Q209L-EE as indicated. (G) Representative images. All micrometer bars, 10 μm. (H) Quantification of SphK1 plasma membrane localization was performed by measuring the fluorescence profiles of individual cells and calculating the plasma membrane/cytosol fluorescence ratios. Each dot represents a single cell. Note: \* *p* < 0.05, \*\*\* *p* < 0.0001 in one-way ANOVA followed by Dunnett’s multiple comparisons test.

Next, we studied plasma membrane translocation of the two mutants in response to  $M_3$  receptor activation in HEK-293 cells. In unstimulated cells, both mCherry-hSphK1-A100E-I101E and mCherry-hSphK1-P104A-L105A were localized in the cytosol of the cells and only a small part was sometimes seen in the nucleus, similar to mCherry-SphK1 wild-type (Figure 6C–E). Interestingly, carbachol-induced translocation of mCherry-hSphK1-A100E-I101E occurred in only 6 of 24 cells (25%), while mCherry-hSphK1 wild-type translocated in 25 of 26 cells (96%) in this set of experiments (Figure 6F). The translocation half-times of mCherry-hSphK1-A100E-I101E in the 6 cells with translocation were not significantly different from those of mCherry-hSphK1 wild-type (Figure 6F). However, translocation efficiency, measured as the % decrease in cytosolic fluorescence, was significantly lower with mCherry-hSphK1-A100E-I101E than with the wild-type enzyme ( $14.0 \pm 2.5\%$ ,  $n = 25$  versus  $23.6 \pm 1.4\%$ ,  $n = 6$ ; mean  $\pm$  SEM; Figure 6D,F). The other mutant, mCherry-hSphK1-P104A-L105A, translocated in 19 of 34 cells stimulated with carbachol (56%), while mCherry-hSphK1 wild-type translocated in 100% of cells in this set of experiments (Figure 6E,F). Again, in the cells which had a response, translocation efficiency of this mutant was significantly reduced ( $16.5 \pm 1.6\%$ ,  $n = 19$  versus  $23.4 \pm 1.5\%$ ,  $n = 16$ ; mean  $\pm$  SEM), while translocation half-times were not significantly different when compared to the wild-type enzyme (Figure 6F). In cells co-transfected with constitutively active  $G\alpha_q$ -Q209L-EE, mCherry-hSphK1-A100E-I101E remained cytosolic in the majority of cells, while mCherry-hSphK1-P104A-L105A was localized at the plasma membrane to a variable extent (Figure 6G). Quantification of the plasma membrane/cytosol fluorescence ratios revealed that  $G\alpha_q$ -Q209L-EE-induced membrane attachment of both mutants was significantly reduced compared to the wild-type enzyme, and that the A100E-I101E mutant was again more affected (Figure 6H). Thus, the results for the two mutants support a role for the AIXXPL motif in  $G_q$  targeting of SphK1.  $G_q$ -mediated translocation was much more strongly affected by mutation of A100 and I101 to glutamate than by mutation of P104 and L105 to alanine. This might be explained by the stronger disruption of the domain by the negative charges of the two glutamates, or by a higher relevance of AI compared to PL. Intriguingly, within the AIXXPL motif, I101 corresponds to L859 in human PLC $\beta_3$  and L475 in human p63RhoGEF, which are most important for  $G_q$  binding [40]. We think that the mutations did not disrupt the general structure of hSphK1, as (1) the molecular weight and subcellular localization in unstimulated cells were normal, (2) both mutants were able to translocate at least in some cells, and (3) S1P concentrations were elevated in cells expressing SphK1-A100E-I101E and SphK1-P104A-L104A indicating catalytic activity. The remaining responses of the mutants might be due to incomplete disruption of the domain, contribution of other parts of the enzyme (see below), or to a second parallel pathway that might involve phosphorylation.

Taken together, we present functional data showing that SphK1 translocation by  $G_{q/11}$ -coupled receptors is prevented by (over)expression of diverse  $G\alpha_{q/11}$  effectors or binding partners, suggesting that SphK1 is targeted either via PLC $\beta$  or directly by activated  $G\alpha_{q/11}$ . The fact that expression of catalytically inactive hSphK1-G82D reduced receptor-stimulated inositol phosphate production argues in favor of the latter possibility, although the role of PLC $\beta$  in this scenario remains unclear. Furthermore, we show that SphK1's conserved AIXXPL motif is involved in translocation of the enzyme by  $G\alpha_q$ . Further studies are required to examine whether this motif indeed mediates direct interaction of SphK1 with  $G\alpha_{q/11}$ . We do not exclude that there are other structural elements in SphK1 that directly or indirectly interact with  $G\alpha_q$ . In fact, we had shown before that both the N-terminus and C-terminus of hSphK1 (except for the TRAF2 binding site) were required for  $M_3$  receptor-induced translocation [23]. The fragment with N-terminal deletion of the first 110 amino acids (hSphK1<sup>111–384</sup>), thus without AIXXPL motif, did not translocate. The fragment with C-terminal deletion of 27 amino acids in addition to the TRAF2 binding site (hSphK1<sup>1–350</sup>) also did not translocate, suggesting that there are other unknown elements in this region required for interaction with  $G\alpha_{q/11}$ , the membrane, or other regulatory proteins (see also discussion in [21]).

There are numerous examples of the importance of SphK1 in  $G_{q/11}$  signaling and functional responses.  $G_{q/11}$ -coupled receptors engaging SphK1 include not only muscarinic receptors [52] and

bradykinin receptors [25], but also protease-activated receptors [53,54], angiotensin receptors [55], or histamine receptors [56,57], just to name a few. These examples show that SphK1 was involved in  $G_{q/11}$ -dependent regulation of the vascular endothelium and smooth muscle,  $G_{q/11}$ -mediated myogenic differentiation of skeletal muscle, or  $G_{q/11}$ -regulated inflammatory responses. From its eminent role in vascular regulation, it was hypothesized recently that SphK1 might be a therapeutic target in pulmonary hypertension [58], in addition to its roles in inflammation, fibrosis, and cancer [10]. Constitutively active  $G_{q/11}$  proteins act as oncogenes [59], and thus given the role of SphK1 in cancer, it will be interesting to unravel a possible interconnection. Another important theme is the emerging role of SphK1 in epithelial–mesenchymal transition [60,61]; however, it should be kept in mind that besides  $G_{q/11}$  proteins, there are many other pathways regulating SphK1 expression and activity, and which may be important in this context. Nevertheless, we strongly believe that unravelling the mechanism(s) by which  $G_{q/11}$  regulates SphK1 will further help to understand the functional roles of this enzyme and facilitate its targeting by potential therapeutics.

**Author Contributions:** Conceptualization, D.M.z.H., T.W.; acquisition of the data, K.V.B., R.F.C., N.J.A., A.K.S., D.M.z.H., S.T., N.F.; resources, J.L.B., J.J.G.T., S.O., T.W., D.M.z.H.; evaluation and discussion of the data, K.V.B., R.F.C., N.J.A., A.K.S., J.J.G.T., S.O., T.W., D.M.z.H.; writing, review and editing, K.V.B., R.F.C., J.J.G.T., T.W., D.M.z.H. All authors have read and agreed to the published version of the manuscript.

**Funding:** This work was funded by the Deutsche Forschungsgemeinschaft (FOG-784; SFB1039 TP A04, B07, and Z01), the LOEWE Lipid Signaling Forschungszentrum Frankfurt (LiFF), and National Institutes of Health grants HL071818 and CA221289 to J.J.G.T.

**Acknowledgments:** We thank Andrea Huwiler (University of Bern, Switzerland) and Josef Pfeilschifter (Goethe-University Frankfurt, Germany) for the SphK1 antibody, and Catherine Berlot (Weis Center for Research, Danville, PA, USA) for the  $G_{\alpha_q}$ -YFP expression plasmid. The expert technical assistance of Luise Reinsberg, Agnes Rudowski, and Nicole Kämpfer-Kolb is gratefully acknowledged.

**Conflicts of Interest:** The authors declare no conflict of interest.

## References

1. Cartier, A.; Hla, T. Sphingosine 1-phosphate: Lipid signaling in pathology and therapy. *Science* **2019**, *366*. [[CrossRef](#)] [[PubMed](#)]
2. Hannun, Y.A.; Obeid, L.M. Sphingolipids and their metabolism in physiology and disease. *Nat. Rev. Mol. Cell Biol.* **2018**, *19*, 175–191. [[CrossRef](#)] [[PubMed](#)]
3. Blaho, V.; Chun, J.; Jonnalagadda, D.; Kihara, Y.; Mizuno, H.; Mpamhanga, C.; Spiegel, S.; Tan, V. Lysophospholipid (S1P) receptors (version 2019.4) in the IUPHAR/BPS Guide to Pharmacology Database. *GtoPdb CITE* **2019**, 2019. [[CrossRef](#)]
4. Shen, H.; Giordano, F.; Wu, Y.; Chan, J.; Zhu, C.; Milosevic, I.; Wu, X.; Yao, K.; Chen, B.; Baumgart, T.; et al. Coupling between endocytosis and sphingosine kinase 1 recruitment. *Nat. Cell Biol.* **2014**, *16*, 652–662. [[CrossRef](#)] [[PubMed](#)]
5. Lima, S.; Milstien, S.; Spiegel, S. Sphingosine and Sphingosine Kinase 1 Involvement in Endocytic Membrane Trafficking. *J. Biol. Chem.* **2017**, *292*, 3074–3088. [[CrossRef](#)]
6. Maceyka, M.; Harikumar, K.B.; Milstien, S.; Spiegel, S. Sphingosine-1-phosphate signaling and its role in disease. *Trends Cell Biol.* **2012**, *22*, 50–60. [[CrossRef](#)]
7. Siow, D.; Wattenberg, B. The compartmentalization and translocation of the sphingosine kinases: Mechanisms and functions in cell signaling and sphingolipid metabolism. *Crit. Rev. Biochem. Mol. Biol.* **2011**, *46*, 365–375. [[CrossRef](#)]
8. Chan, H.; Pitson, S.M. Post-translational regulation of sphingosine kinases. *Biochim. Biophys. Acta* **2013**, *1831*, 147–156. [[CrossRef](#)]
9. Pulkoski-Gross, M.J.; Obeid, L.M. Molecular mechanisms of regulation of sphingosine kinase 1. *Biochim. Biophys. Acta Mol. Cell Biol. Lipids* **2018**, *1863*, 1413–1422. [[CrossRef](#)]
10. Pyne, S.; Adams, D.R.; Pyne, N.J. Sphingosine Kinases as Druggable Targets. *Handb. Exp. Pharmacol.* **2018**. [[CrossRef](#)]

11. Hobson, J.P.; Rosenfeldt, H.M.; Barak, L.S.; Olivera, A.; Poulton, S.; Caron, M.G.; Milstien, S.; Spiegel, S. Role of the sphingosine-1-phosphate receptor EDG-1 in PDGF-induced cell motility. *Science* **2001**, *291*, 1800–1803. [[CrossRef](#)] [[PubMed](#)]
12. Spiegel, S.; Maczys, M.A.; Maceyka, M.; Milstien, S. New insights into functions of the sphingosine-1-phosphate transporter SPNS2. *J. Lipid Res.* **2019**, *60*, 484–489. [[CrossRef](#)] [[PubMed](#)]
13. Johnson, K.R.; Becker, K.P.; Facchinetti, M.M.; Hannun, Y.A.; Obeid, L.M. PKC-dependent activation of sphingosine kinase 1 and translocation to the plasma membrane. Extracellular release of sphingosine-1-phosphate induced by phorbol 12-myristate 13-acetate (PMA). *J. Biol. Chem.* **2002**, *277*, 35257–35262. [[CrossRef](#)] [[PubMed](#)]
14. Pitson, S.M.; Moretti, P.A.B.; Zebol, J.R.; Lynn, H.E.; Xia, P.; Vadas, M.A.; Wattenberg, B.W. Activation of sphingosine kinase 1 by ERK1/2-mediated phosphorylation. *EMBO J.* **2003**, *22*, 5491–5500. [[CrossRef](#)] [[PubMed](#)]
15. Gault, C.R.; Eblen, S.T.; Neumann, C.A.; Hannun, Y.A.; Obeid, L.M. Oncogenic K-Ras regulates bioactive sphingolipids in a sphingosine kinase 1-dependent manner. *J. Biol. Chem.* **2012**, *287*, 31794–31803. [[CrossRef](#)]
16. Jarman, K.E.; Moretti, P.A.B.; Zebol, J.R.; Pitson, S.M. Translocation of sphingosine kinase 1 to the plasma membrane is mediated by calcium- and integrin-binding protein 1. *J. Biol. Chem.* **2010**, *285*, 483–492. [[CrossRef](#)]
17. Delon, C.; Manifava, M.; Wood, E.; Thompson, D.; Krugmann, S.; Pyne, S.; Ktistakis, N.T. Sphingosine kinase 1 is an intracellular effector of phosphatidic acid. *J. Biol. Chem.* **2004**, *279*, 44763–44774. [[CrossRef](#)]
18. Pulkoski-Gross, M.J.; Jenkins, M.L.; Truman, J.-P.; Salama, M.F.; Clarke, C.J.; Burke, J.E.; Hannun, Y.A.; Obeid, L.M. An intrinsic lipid-binding interface controls sphingosine kinase 1 function. *J. Lipid Res.* **2018**, *59*, 462–474. [[CrossRef](#)]
19. Wang, J.; Knapp, S.; Pyne, N.J.; Pyne, S.; Elkins, J.M. Crystal Structure of Sphingosine Kinase 1 with PF-543. *ACS Med. Chem. Lett.* **2014**, *5*, 1329–1333. [[CrossRef](#)]
20. Wang, Z.; Min, X.; Xiao, S.-H.; Johnstone, S.; Romanow, W.; Meiningner, D.; Xu, H.; Liu, J.; Dai, J.; An, S.; et al. Molecular basis of sphingosine kinase 1 substrate recognition and catalysis. *Structure* **2013**, *21*, 798–809. [[CrossRef](#)]
21. Adams, D.R.; Pyne, S.; Pyne, N.J. Sphingosine Kinases: Emerging Structure-Function Insights. *Trends Biochem. Sci.* **2016**, *41*, 395–409. [[CrossRef](#)] [[PubMed](#)]
22. Alemany, R.; van Koppen, C.J.; Danneberg, K.; ter Braak, M.; Meyer zu Heringdorf, D. Regulation and functional roles of sphingosine kinases. *Naunyn Schmiedebergs. Arch. Pharmacol.* **2007**, *374*, 413–428. [[CrossRef](#)] [[PubMed](#)]
23. ter Braak, M.; Danneberg, K.; Lichte, K.; Liphardt, K.; Ktistakis, N.T.; Pitson, S.M.; Hla, T.; Jakobs, K.H.; Meyer zu Heringdorf, D. G $\alpha$ (q)-mediated plasma membrane translocation of sphingosine kinase-1 and cross-activation of S1P receptors. *Biochim. Biophys. Acta* **2009**, *1791*, 357–370. [[CrossRef](#)] [[PubMed](#)]
24. Blankenbach, K.V.; Bruno, G.; Wondra, E.; Spohner, A.K.; Aster, N.J.; Vienken, H.; Trautmann, S.; Ferreirós, N.; Wieland, T.; Bruni, P.; et al. The WD40 repeat protein, WDR36, orchestrates sphingosine kinase-1 recruitment and phospholipase C- $\beta$  activation by Gq-coupled receptors. *Biochim. Biophys. Acta Mol. Cell Biol. Lipids* **2020**, *1865*, 158704. [[CrossRef](#)] [[PubMed](#)]
25. Bruno, G.; Cencetti, F.; Bernacchioni, C.; Donati, C.; Blankenbach, K.V.; Thomas, D.; Meyer zu Heringdorf, D.; Bruni, P. Bradykinin mediates myogenic differentiation in murine myoblasts through the involvement of SK1/Spns2/S1P2 axis. *Cell. Signal.* **2018**, *45*, 110–121. [[CrossRef](#)] [[PubMed](#)]
26. Vienken, H.; Mabrouki, N.; Grabau, K.; Claas, R.F.; Rudowski, A.; Schömel, N.; Pfeilschifter, J.; Lütjohann, D.; van Echten-Deckert, G.; Meyer zu Heringdorf, D. Characterization of cholesterol homeostasis in sphingosine-1-phosphate lyase-deficient fibroblasts reveals a Niemann-Pick disease type C-like phenotype with enhanced lysosomal Ca<sup>2+</sup> storage. *Sci. Rep.* **2017**, *7*. [[CrossRef](#)]
27. Kostenis, E.; Martini, L.; Ellis, J.; Waldhoer, M.; Heydorn, A.; Rosenkilde, M.M.; Norregaard, P.K.; Jorgensen, R.; Whistler, J.L.; Milligan, G. A highly conserved glycine within linker I and the extreme C terminus of G protein alpha subunits interact cooperatively in switching G protein-coupled receptor-to-effector specificity. *J. Pharmacol. Exp. Ther.* **2005**, *313*, 78–87. [[CrossRef](#)]

28. Hughes, T.E.; Zhang, H.; Logothetis, D.E.; Berlot, C.H. Visualization of a functional Galpha q-green fluorescent protein fusion in living cells. Association with the plasma membrane is disrupted by mutational activation and by elimination of palmitoylation sites, but not by activation mediated by receptors or AIF4-. *J. Biol. Chem.* **2001**, *276*, 4227–4235. [[CrossRef](#)]
29. Carman, C.V.; Parent, J.L.; Day, P.W.; Pronin, A.N.; Sternweis, P.M.; Wedegaertner, P.B.; Gilman, A.G.; Benovic, J.L.; Kozasa, T. Selective regulation of Galpha(q/11) by an RGS domain in the G protein-coupled receptor kinase, GRK2. *J. Biol. Chem.* **1999**, *274*, 34483–34492. [[CrossRef](#)]
30. Sterne-Marr, R.; Tesmer, J.J.G.; Day, P.W.; Stracquatano, R.P.; Cilente, J.-A.E.; O'Connor, K.E.; Pronin, A.N.; Benovic, J.L.; Wedegaertner, P.B. G protein-coupled receptor Kinase 2/G alpha q/11 interaction. A novel surface on a regulator of G protein signaling homology domain for binding G alpha subunits. *J. Biol. Chem.* **2003**, *278*, 6050–6058. [[CrossRef](#)]
31. Tesmer, V.M.; Kawano, T.; Shankaranarayanan, A.; Kozasa, T.; Tesmer, J.J.G. Snapshot of activated G proteins at the membrane: The Galphaq-GRK2-Gbetagamma complex. *Science* **2005**, *310*, 1686–1690. [[CrossRef](#)] [[PubMed](#)]
32. Moepps, B.; Tulone, C.; Kern, C.; Minisini, R.; Michels, G.; Vatter, P.; Wieland, T.; Gierschik, P. Constitutive serum response factor activation by the viral chemokine receptor homologue pUS28 is differentially regulated by Galpha(q/11) and Galpha(16). *Cell. Signal.* **2008**, *20*, 1528–1537. [[CrossRef](#)] [[PubMed](#)]
33. Shankaranarayanan, A.; Boguth, C.A.; Lutz, S.; Vettel, C.; Uhlemann, F.; Aittaleb, M.; Wieland, T.; Tesmer, J.J.G. Galpha q allosterically activates and relieves autoinhibition of p63RhoGEF. *Cell. Signal.* **2010**, *22*, 1114–1123. [[CrossRef](#)] [[PubMed](#)]
34. van Unen, J.; Reinhard, N.R.; Yin, T.; Wu, Y.I.; Postma, M.; Gadella, T.W.J.; Goedhart, J. Plasma membrane restricted RhoGEF activity is sufficient for RhoA-mediated actin polymerization. *Sci. Rep.* **2015**, *5*, 14693. [[CrossRef](#)]
35. Sinnecker, D.; Schaefer, M. Real-time analysis of phospholipase C activity during different patterns of receptor-induced Ca<sup>2+</sup> responses in HEK293 cells. *Cell Calcium* **2004**, *35*, 29–38. [[CrossRef](#)]
36. Freeman, T.C.; Black, J.L.; Bray, H.G.; Dagliyan, O.; Wu, Y.I.; Tripathy, A.; Dokholyan, N.V.; Leisner, T.M.; Parise, L.V. Identification of novel integrin binding partners for calcium and integrin binding protein 1 (CIB1): Structural and thermodynamic basis of CIB1 promiscuity. *Biochemistry* **2013**, *52*, 7082–7090. [[CrossRef](#)]
37. Black, J.L.; Harrell, J.C.; Leisner, T.M.; Fellmeth, M.J.; George, S.D.; Reinhold, D.; Baker, N.M.; Jones, C.D.; Der, C.J.; Perou, C.M.; et al. CIB1 depletion impairs cell survival and tumor growth in triple-negative breast cancer. *Breast Cancer Res. Treat.* **2015**, *152*, 337–346. [[CrossRef](#)]
38. Offermanns, S.; Zhao, L.P.; Gohla, A.; Sarosi, I.; Simon, M.I.; Wilkie, T.M. Embryonic cardiomyocyte hypoplasia and craniofacial defects in G alpha q/G alpha 11-mutant mice. *EMBO J.* **1998**, *17*, 4304–4312. [[CrossRef](#)]
39. Döll, F.; Pfeilschifter, J.; Huwiler, A. The epidermal growth factor stimulates sphingosine kinase-1 expression and activity in the human mammary carcinoma cell line MCF7. *Biochim. Biophys. Acta* **2005**, *1738*, 72–81. [[CrossRef](#)]
40. Lyon, A.M.; Taylor, V.G.; Tesmer, J.J.G. Strike a pose: Gαq complexes at the membrane. *Trends Pharmacol. Sci.* **2014**, *35*, 23–30. [[CrossRef](#)]
41. Lutz, S.; Freichel-Blomquist, A.; Yang, Y.; Rumenapp, U.; Jakobs, K.H.; Schmidt, M.; Wieland, T. The guanine nucleotide exchange factor p63RhoGEF, a specific link between Gq/11-coupled receptor signaling and RhoA. *J. Biol. Chem.* **2005**, *280*, 11134–11139. [[CrossRef](#)] [[PubMed](#)]
42. Lutz, S.; Shankaranarayanan, A.; Coco, C.; Ridilla, M.; Nance, M.R.; Vettel, C.; Baltus, D.; Evelyn, C.R.; Neubig, R.R.; Wieland, T.; et al. Structure of Galphaq-p63RhoGEF-RhoA complex reveals a pathway for the activation of RhoA by GPCRs. *Science* **2007**, *318*, 1923–1927. [[CrossRef](#)] [[PubMed](#)]
43. Watt, S.A.; Kular, G.; Fleming, I.N.; Downes, C.P.; Lucocq, J.M. Subcellular localization of phosphatidylinositol 4,5-bisphosphate using the pleckstrin homology domain of phospholipase C delta1. *Biochem. J.* **2002**, *363*, 657–666. [[CrossRef](#)] [[PubMed](#)]
44. Szymańska, E.; Sobota, A.; Czuryło, E.; Kwiatkowska, K. Expression of PI(4,5)P<sub>2</sub>-binding proteins lowers the PI(4,5)P<sub>2</sub> level and inhibits FcγRIIA-mediated cell spreading and phagocytosis. *Eur. J. Immunol.* **2008**, *38*, 260–272. [[CrossRef](#)] [[PubMed](#)]

45. Weernink, P.A.O.; Meletiadiis, K.; Hommeltenberg, S.; Hinz, M.; Ishihara, H.; Schmidt, M.; Jakobs, K.H. Activation of type I phosphatidylinositol 4-phosphate 5-kinase isoforms by the Rho GTPases, RhoA, Rac1, and Cdc42. *J. Biol. Chem.* **2004**, *279*, 7840–7849. [[CrossRef](#)]
46. Rügenapp, U.; Schmidt, M.; Olesch, S.; Ott, S.; Eichel-Streiber, C.V.; Jakobs, K.H. Tyrosine-phosphorylation-dependent and rho-protein-mediated control of cellular phosphatidylinositol 4,5-bisphosphate levels. *Biochem. J.* **1998**, *334 Pt 3*, 625–631. [[CrossRef](#)]
47. Pitson, S.M.; Moretti, P.A.; Zebol, J.R.; Xia, P.; Gamble, J.R.; Vadas, M.A.; D’andrea, R.J.; Wattenberg, B.W. Expression of a catalytically inactive sphingosine kinase mutant blocks agonist-induced sphingosine kinase activation. A dominant-negative sphingosine kinase. *J. Biol. Chem.* **2000**, *275*, 33945–33950. [[CrossRef](#)]
48. Day, P.W.; Tesmer, J.J.G.; Sterne-Marr, R.; Freeman, L.C.; Benovic, J.L.; Wedegaertner, P.B. Characterization of the GRK2 binding site of Galphaq. *J. Biol. Chem.* **2004**, *279*, 53643–53652. [[CrossRef](#)]
49. Venkatakrishnan, G.; Exton, J.H. Identification of determinants in the alpha-subunit of Gq required for phospholipase C activation. *J. Biol. Chem.* **1996**, *271*, 5066–5072. [[CrossRef](#)]
50. Sutherland, C.M.; Moretti, P.A.B.; Hewitt, N.M.; Bagley, C.J.; Vadas, M.A.; Pitson, S.M. The calmodulin-binding site of sphingosine kinase and its role in agonist-dependent translocation of sphingosine kinase 1 to the plasma membrane. *J. Biol. Chem.* **2006**, *281*, 11693–11701. [[CrossRef](#)]
51. Inagaki, Y.; Li, P.-Y.; Wada, A.; Mitsutake, S.; Igarashi, Y. Identification of functional nuclear export sequences in human sphingosine kinase 1. *Biochem. Biophys. Res. Commun.* **2003**, *311*, 168–173. [[CrossRef](#)] [[PubMed](#)]
52. Mulders, A.C.M.; Mathy, M.-J.; Meyer zu Heringdorf, D.; ter Braak, M.; Hajji, N.; Olthof, D.C.; Michel, M.C.; Alewijnse, A.E.; Peters, S.L.M. Activation of sphingosine kinase by muscarinic receptors enhances NO-mediated and attenuates EDHF-mediated vasorelaxation. *Basic Res. Cardiol.* **2009**, *104*, 50–59. [[CrossRef](#)] [[PubMed](#)]
53. Billich, A.; Urtz, N.; Reuschel, R.; Baumruker, T. Sphingosine kinase 1 is essential for proteinase-activated receptor-1 signalling in epithelial and endothelial cells. *Int. J. Biochem. Cell Biol.* **2009**, *41*, 1547–1555. [[CrossRef](#)]
54. Böhm, A.; Flößer, A.; Ermler, S.; Fender, A.C.; Lüth, A.; Kleuser, B.; Schrör, K.; Rauch, B.H. Factor-Xa-induced mitogenesis and migration require sphingosine kinase activity and S1P formation in human vascular smooth muscle cells. *Cardiovasc. Res.* **2013**, *99*, 505–513. [[CrossRef](#)]
55. Siedlinski, M.; Nosalski, R.; Szczepaniak, P.; Ludwig-Gałęzowska, A.H.; Mikołajczyk, T.; Filip, M.; Osmenda, G.; Wilk, G.; Nowak, M.; Wołkow, P.; et al. Vascular transcriptome profiling identifies Sphingosine kinase 1 as a modulator of angiotensin II-induced vascular dysfunction. *Sci. Rep.* **2017**, *7*, 44131. [[CrossRef](#)] [[PubMed](#)]
56. Huwiler, A.; Döll, F.; Ren, S.; Klawitter, S.; Greening, A.; Römer, I.; Bubnova, S.; Reinsberg, L.; Pfeilschifter, J. Histamine increases sphingosine kinase-1 expression and activity in the human arterial endothelial cell line EA.hy 926 by a PKC-alpha-dependent mechanism. *Biochim. Biophys. Acta* **2006**, *1761*, 367–376. [[CrossRef](#)]
57. Sun, W.Y.; Abeynaike, L.D.; Escarbe, S.; Smith, C.D.; Pitson, S.M.; Hickey, M.J.; Bonder, C.S. Rapid histamine-induced neutrophil recruitment is sphingosine kinase-1 dependent. *Am. J. Pathol.* **2012**, *180*, 1740–1750. [[CrossRef](#)]
58. Pyne, N.J.; Pyne, S. Sphingosine Kinase 1: A Potential Therapeutic Target in Pulmonary Arterial Hypertension? *Trends Mol. Med.* **2017**, *23*, 786–798. [[CrossRef](#)]
59. Kostenis, E.; Pfeil, E.M.; Annala, S. Heterotrimeric Gq proteins as therapeutic targets? *J. Biol. Chem.* **2020**, *295*, 5206–5215. [[CrossRef](#)]
60. Meshcheryakova, A.; Svoboda, M.; Tahir, A.; Köfeler, H.C.; Triebl, A.; Mungenast, F.; Heinze, G.; Gerner, C.; Zimmermann, P.; Jaritz, M.; et al. Exploring the role of sphingolipid machinery during the epithelial to mesenchymal transition program using an integrative approach. *Oncotarget* **2016**, *7*, 22295–22323. [[CrossRef](#)]
61. Liu, S.-Q.; Xu, C.-Y.; Wu, W.-H.; Fu, Z.-H.; He, S.-W.; Qin, M.-B.; Huang, J.-A. Sphingosine kinase 1 promotes the metastasis of colorectal cancer by inducing the epithelial-mesenchymal transition mediated by the FAK/AKT/MMPs axis. *Int. J. Oncol.* **2019**, *54*, 41–52. [[CrossRef](#)] [[PubMed](#)]

